

ShiftedBronzes: Benchmarking and Analysis of Domain Fine-Grained Classification in Open-World Settings

Rixin Zhou¹ Honglin Pang¹ Qian Zhang³ Ruihua Qi³ Xi Yang^{1,2,*} Chuntao Li^{3,*}

¹School of Artificial Intelligence, Jilin University

²Engineering Research Center of Knowledge-Driven Human-Machine Intelligence, MoE, China

³School of Archaeology, Jilin University



Figure 1. Examples of our proposed dataset and a general OOD dataset (OpenImage-O [94]). Our dataset include 2 types of ID data (a-b) and 7 types OOD data (c-i). (a) and (b) are typical images of bronze Ding and Gui from four dynasties (Shang, Western Zhou, Spring and Autumn, Warring States), which together form the ID data for the bronze ware dating task. (c-f) are sketch images and rubbing images of Ding and Gui. (g) and (h) are generated images by applying a zero-shot material transfer model to bronze ware and container images. (i) are container images sourced from the ImageNet-21K [74] dataset. (j) are examples from OpenImage-O. In terms of bronze ware dating scenarios, the distribution shift between the ID data and the OOD data increases from left to right within the green region.

Abstract

In real-world applications across specialized domains, addressing complex out-of-distribution (OOD) challenges is a common and significant concern. In this study, we concentrate on the task of fine-grained bronze ware dating, a critical aspect in the study of ancient Chinese history, and developed a benchmark dataset named ShiftedBronzes. By extensively expanding the bronze Ding dataset [111], ShiftedBronzes incorporates two types of bronze ware data and seven types of OOD data, which exhibit distribution shifts commonly encountered in bronze ware dating scenarios. We conduct benchmarking experiments on ShiftedBronzes and five commonly used general OOD datasets, employing a variety of widely adopted post-hoc, pre-trained Vision Large

Model (VLM)-based and generation-based OOD detection methods. Through analysis of the experimental results, we validate previous conclusions regarding post-hoc, VLM-based, and generation-based methods, while also highlighting their distinct behaviors on specialized datasets. These findings underscore the unique challenges of applying general OOD detection methods to domain-specific tasks such as bronze ware dating. We hope that the ShiftedBronzes benchmark provides valuable insights into both the field of bronze ware dating and the development of OOD detection methods. The dataset and associated code will be available later.

*Corresponding authors

1. Introduction

In practical applications within the open world, specialized domains often encounter complex out-of-distribution (OOD) issues. Most existing fine-grained visual classification (FGVC) methods, including those for bronze ware dating, are trained based on the closed-world assumption [34, 46], where the test data is assumed to be drawn independent and identically distributed (i.i.d.) from the same distribution as the training data. In contrast with general OOD benchmarks [55, 100, 107] on ImageNet classification, the domain fine-grained benchmarks are limited. Studies on OOD benchmarks have been proposed for specific areas of expertise, such as materials property prediction [72], drug discovery [44] and medical image [10]. However, these domain-specific OOD benchmarks focus more on the development of their own fields, lacking consideration of how domain-specific data could advance OOD detection methods. Additionally, there is a lack of benchmark research on the archaeological dating of bronze wares in open-world settings.

To fill this gap and advance the development of bronze ware dating in open-world scenarios, we constructed a comprehensive benchmark ShiftedBronzes for bronze ware dating by significantly expanded the existing bronze Ding dataset [111]. The ShiftedBronzes dataset consists of seven data components, identified as Ding, Gui, Ding sketch, Gui sketch, Ding rubbing, Gui rubbing, transferred container, transferred bronze, container. Figure 1 illustrates examples from our proposed dataset alongside samples from a general OOD dataset, OpenImage-O [94]. In the bronze ware dating task, Ding and Gui data act as in-distribution (ID) data, while the remaining data types are OOD. There are a total of 6,208 color, sketch, and rubbing images of Ding and Gui. All expanded bronze ware data have been thoroughly annotated with expert knowledge. There are 51,023 images for the transferred container, transferred bronze, and container, respectively.

The characteristics of our dataset are as follows. As illustrated in the green OOD region of Figure 1, the distribution shift between the bronze ware ID data and the OOD data gradually increases from left to right. These data correspond to different types of distribution shift encountered in the bronze ware dating scenario. Among the OOD data, sketch and rubbing images are specialized types of data commonly encountered in archaeological contexts. Sketches capture the shape and decoration of bronze wares, while rubbings use ink to transfer three-dimensional details onto a flat surface. These two types of specialized images exhibit smaller distribution shifts compared to other OOD data types, which makes them more similar to the bronze ware ID data in terms of appearance and structure. Generated bronze images simulate the material properties of real bronze ware and are used to represent unknown types of

bronze wares in the context of bronze ware dating. Similarly, generated container images depict craft items that resemble the shapes of bronze wares, posing challenges in distinguishing them from genuine bronze ware. Given that both Ding and Gui function as containers, modern container images further complicate the task of bronze ware dating by introducing additional visual noise.

Based on ShiftedBronzes and five general OOD datasets, we benchmark six representative FGVC methods in the bronze ware dating task and eighteen representative OOD detection methods in the bronze ware OOD detection task. Our evaluation of the FGVC methods in the bronze ware dating task aligns with settings specifically designed for bronze Ding dating [111]. The OOD detection methods we selected can be classified into three categories: post-hoc-based, pretrained vision language models (VLMs)-based, and generation-based methods.

The OOD detection experiments conducted on ShiftedBronzes not only reaffirm established conclusions from general OOD data but also provide new insights specific to OOD detection in specialized datasets. Compared to general OOD data, current methods face greater challenges when detecting domain-specific OOD samples with small distribution shifts. Among the methods compared, VLM-based methods consistently outperform both post-hoc and generation-based methods. By analyzing the performance differences among various VLM-based methods, we uncover the factors contributing to their superior performance in both domain-specific and general OOD detection, while also revealing distinct ID-OOD correlations in specialized versus general domains. The top-performing post-hoc methods highlight critical factors influencing OOD detection, suggesting directions for future improvements in post-hoc techniques. Additionally, pre-trained diffusion model-based methods demonstrate a clear advantage in detecting OOD samples from the sketch and rubbing categories compared to other OOD data types.

The main contributions are summarized below:

- We propose ShiftedBronzes, a comprehensive benchmark designed for evaluating bronze ware dating and OOD detection methods in scenarios characterized by diverse real-world domain distribution shifts.
- We benchmark six representative FGVC methods for the bronze ware dating task and classify eighteen representative OOD detection methods into three categories for evaluation in the bronze ware OOD detection task.
- A comprehensive analysis of the experimental results led to conclusions that contribute to both bronze ware dating research and the development of OOD detection methods.

2. Related Work

2.1. OOD Benchmark

Currently, numerous OOD benchmarks have been proposed to assess and compare the performance of various algorithms, models, or systems. OpenOOD [100] categorizes OOD datasets into different difficulties, and establishes multiple benchmarks to provide a comprehensive evaluation of various OOD detection methods. Benchmark studies on OOD detection have been initiated for specific areas of expertise. Omeo et al. [72] conducted a benchmarking analysis to evaluate the robustness of structure-based graph neural networks in the context of predicting properties of OOD materials. Ji et al. [44] present a systematic OOD dataset curator and benchmark for AI-aided drug discovery. Cao et al. [10] undertake a benchmarking analysis of prevalent OOD detection methods across three pivotal areas of medical imaging. Studies on the robustness of OOD detection [55, 64, 107] benchmark the performance of OOD methods under various distribution shifts by introducing perturbation variables into images. However, existing domain-specific OOD benchmarks primarily focus on advancing their respective fields, without addressing how domain-specific data can enhance OOD detection methods. Furthermore, there is a notable absence of benchmark research on the archaeological dating of bronze wares within open-world scenarios.

2.2. OOD Detection Methods

OOD detection is a crucial task in computer vision, vital for ensuring robust model performance in real-world applications. This challenge has attracted considerable research, with a particular emphasis on post-hoc methods and those based on Vision-Language Models (VLMs). These approaches are favored due to their practical advantages, including ease of implementation and relevance to real-world use cases. Among the studies on post-hoc OOD detection methods, Hendrycks et al. [37] proposed a baseline OOD detection method using the maximum softmax probability (MSP) as an ID score. Subsequent studies have investigated alternative, efficient indicators to differentiate between ID and OOD samples, such as gradient-based methods [39, 56], mahalanobis distance-based method [51], energy-based functions [59], gram matrix-based method [78] and weight sparsification-based method [89]. Among the studies on VLM-based OOD detection methods, Ming et al. [65] have extended the MSP score to VLM, examining the effects of softmax probabilities and temperature scaling on OOD detection performance. LoCoOp [69] performs OOD regularization that utilizes the portions of CLIP [73] local features as OOD features during training. CLIPN [93] fine-tuned CLIP to enable it to output negative prompts to assess the probability

of a OOD concept. ID-like [5] explore ID-like OOD samples in the vicinity space of ID samples leveraging CLIP and utilizing prompt learning framework to identify ID-like outliers to further leverage the capabilities of CLIP for OOD detection.

Generation-based OOD detection methods also represent a significant research focus. GANs have been used to synthesize unknown samples from known classes, aiding in distinguishing between known and unknown samples for open set recognition [45, 110] and OOD detection [86, 92]. Some methods prioritize reconstruction quality from input data [79] or estimate data density via generative models [80]. Recent research has utilized diffusion models for detecting OOD and novelty instances [30, 67]. For example, DIFFGUARD [27] applies diffusion models to detect OOD instances with semantic discrepancies by conditioning generation on both input images and semantic labels. Additionally, Du et al. [23] leverages a diffusion model to produce high-resolution, realistic outliers, enhancing a model’s capacity to identify unknown inputs during deployment.

2.3. Bronze Ware Dating

Bronze ware dating task aims at determining the specific historical age to which the bronze ware belongs. The chemical and physical properties of metals are used to locate the exact year of a bronze ware [19, 20, 58, 96]. Zhou et al. [111] consider the dating of bronze Ding as a fine-grained classification problem and examine several FGVC methods [13, 14, 41, 101, 102] to address the bronze ware dating task. They also collected a dataset of bronze Ding and developed a multi-granularity bronze ware dating model. Furthermore, the research in [52] has established an online mini-program platform designed to recognize the eras of bronze Ding. However, current methods are based on the i.i.d. assumption, making it challenging to handle OOD input samples in open-world scenarios.

3. ShiftedBronzes Benchmark

Our goal is to establish a comprehensive benchmark specifically tailored to real-world scenarios in bronze ware dating. To achieve this, we have curated two types of bronze ware data and seven types of OOD data that reflect common distribution shifts encountered in this domain.

The bronze ware data includes color images of Ding and Gui, which serve as the ID data used to train FGVC methods for bronze ware dating. This data is split into training, validation, and test sets, as detailed in Section 4.1. Additionally, we include sketch and rubbing images, which are professional representations of bronze ware forms, patterns, and inscriptions, captured using specialized techniques. These images are commonly used in the context of bronze ware dating. The ”Transferred container data” consists of im-

ages simulating other categories of bronze wares or counterfeit items, while "Transferred bronze data" mimics artificial craft items that resemble bronze wares in shape. Containers, sharing functional similarities with bronze wares, are often mistaken for them, which makes distinguishing between these categories challenge in the context of OOD detection.

Table 1. Statistics of bronze ware, sketch, rubbing and transferred container data.

Era	Shang		Western Zhou			Spring and Autumn			Warring States			Total
	Early	Late	Early	Mid	Late	Early	Mid	Late	Early	Mid	Late	
Bronze Ware Data (ID)												
Ding	93	945	801	410	264	298	189	215	85	78	141	3519
Gui	8	355	732	550	352	138	16	27	8	5	1	2192
Sketch, Rubbing and Transferred Container Data (OOD)												
Ding Sketch and Rubbing	0	67	51	18	15	4	4	2	2	0	8	171
Gui Sketch and Rubbing	0	46	113	72	78	14	2	0	0	0	1	326
Transferred Container	918	11718	13805	8166	5544	3924	1854	2196	846	756	1296	51023

3.1. Bronze Ware, Sketch and Rubbing Data

Data Collection. We divide the bronze Ding dataset [111] into three categories: color, sketch, and rubbing images of bronze ware. To expand these datasets, we collect and annotate 2518 Gui images from both five published archaeology books and four websites, which are also organized into color, sketch, and rubbing categories. The quantitative statistics of Ding and Gui dataset are presented in Table 1.

Data Annotation. All bronze Gui have been annotated with comprehensive expert knowledge, including era (4 course-grained dynasties and 11 fine-grained periods), attributes (35 shapes and 149 characteristics with bounding boxes), literature, locations of excavation, and current exhibition museums. The numbers of shapes and characteristics labels are shown in Figure 2 (a). Because many dating results are controversial, we re-argue the era of each artifact through discussions with three bronze experts. The collection and labelling of data were carried out by an archaeologist and eight archaeology assists, who took approximately eight months to complete.

3.2. Container Data

Data Collection. As shown in Figure 3, the process of collecting container data can be divided into three steps: **Step 1:** We employed an open-source large language model [70] to sift through the 21,841 categories of ImageNet-21K, selecting those that are related to the concept of containers, such as "bowl", "cup" and others. A total of 94 categories related to the concept of containers were identified, encompassing 76399 images; **Step 2:** We removed those categories that appeared in the ImageNet-1K dataset, leaving 83 categories; **Step 3:** We removed images in which the containers are secondary instances, such as a person holding a wine glass or a baby with a bottle, leaving 51,023 container images. The statistics of the container categories is illustrated in Figure 2 (b).

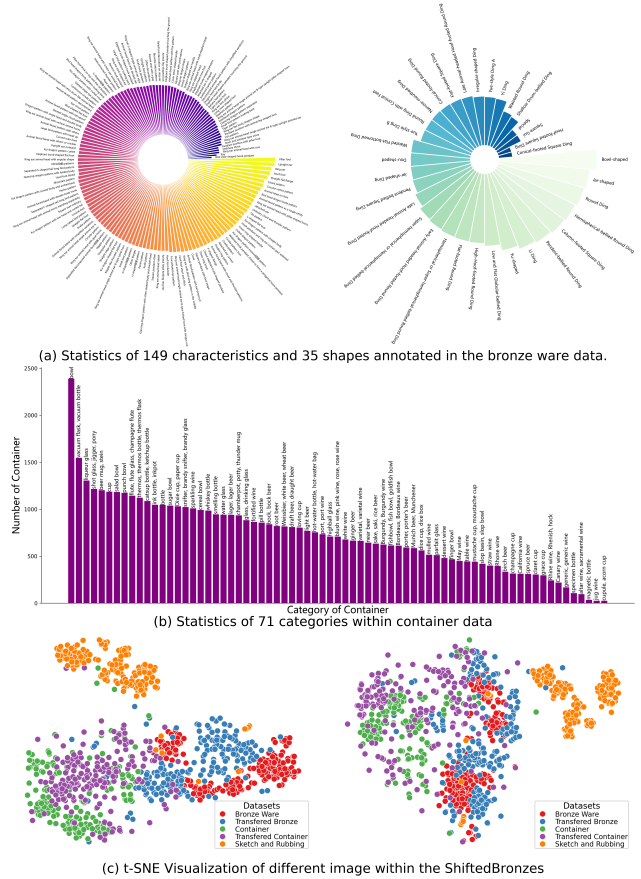


Figure 2. (a) Statistical of expert-annotated knowledge within the bronze ware dataset. (b) Statistics of categories within container data. (c) Feature visualization of different image within the ShiftedBronzes. Features are extracted using ResNet-50 (left) and ViT-B-16 (right) models, both pre-trained on the ImageNet-1K dataset, followed by dimensionality reduction via t-SNE.

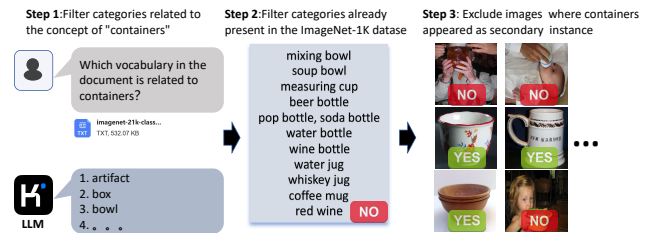


Figure 3. The detailed process for collecting container data.

3.3. Transferred OOD Data

Transferred Container Data. By transferring the materials of bronze wares onto containers, we can obtain 51,023 transferred container data that combine the material characteristics of bronze wares with the shapes of modern containers, as shown in Figure 4 (a). To prevent information leakage from the training data, we used 2861 bronze ware

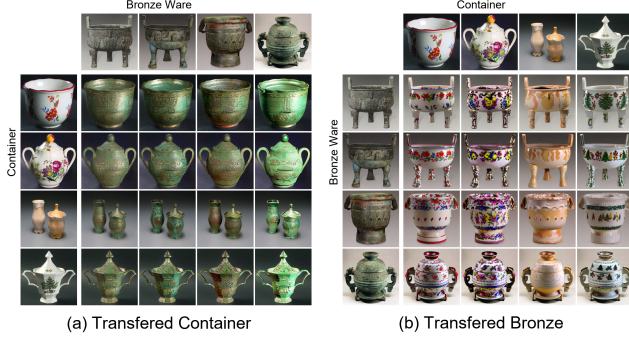


Figure 4. The generation process of transferred container and transferred bronze data using the zero-shot material transfer model ZeST [16].

images from the test set to perform material transfers on 51023 container images, with an average of 17 container images corresponding to each bronze ware image. Consequently, the transferred container data can also be correlated with each era based on the corresponding bronze ware images. The era statistics for the transferred container data are presented in Table 1.

Transferred Bronze Data. By transferring the materials of modern containers onto bronze wares, we can obtain 51,023 transferred bronze data that combine the material characteristics of containers with the shapes of bronze wares, as illustrated in Figure 4 (b). We used 51023 container images to perform material transfers on the 2861 bronze ware test data. The statistics of transferred bronze data are consistent with those of the container data shown in Figure 2 (b).

3.4. Distribution Shift Analysis

To analyze the distribution of different data in Shifted-Bronzes, we randomly selected 200 images from each data type: bronze ware images, transferred bronze images, container images, transferred container images, sketch and rubbing images. We used the ResNet-50 [36] and ViT-B/16 [21] models pre-trained on ImageNet-1K to extract image features, then applied t-SNE for feature dimensionality reduction, and finally visualized the reduced features, as shown in Figure 2 (c). The feature gaps of sketch and rubbing images, bronze ware images, transferred bronze images, transferred container images, and container images are relatively small, indicating that their distances in the original space are close, suggesting potential difficulties in distinguishing them.

4. Experiments

4.1. Data Preparation

The bronze ware data from our proposed ShiftedBronzes is used as ID data to train the bronze ware dating methods. Following the divisions of bronze Ding dataset [111] and other fine-grained classification datasets [61, 111], we split the 5711 bronze Ding and Gui images into three sets: the scales of the training set, validation set, and test set are 4:1:5 (2278:572:2861), respectively. And each fine-grained period and bronze ware category is split following this ratio.

Besides the ShiftedBronzes OOD data, we additionally utilized five general OOD datasets from ImageNet-1K, including Species [6], ImageNet-O [38], iNaturalist [40], Texture [48], and OpenImage-O [94]. Considering the degree of distribution shift from the ID data, we classified the seven OOD data types in ShiftedBronzes as *hard OOD data* and the five general OOD datasets as *easy OOD data*.

4.2. Implementation Details

Devices and Code. All experiments were implemented by PyTorch, and conducted on a server with 4 RTX A40 GPUs and Intel® Xeon® Gold 5220 CPUs (72 cores). The code for all post-hoc OOD detection methods and OpenGAN method are derived from openOOD benchmark [100]. And the code for other methods are derived from the corresponding official repositories. The hyperparameters for each method are set according to the optimal configurations reported in their respective papers.

Evaluation. For evaluation metrics, we employ FPR@95 and AUROC for the OOD detection task and OA and accuracy for the dating task. AUROC is a metric that computes the area under the receiver operating characteristic curve. A higher value indicates better detection performance. FPR@95 is short for FPR@TPR95, which is the false positive rate when the true positive rate is 95%. Smaller FPR@95 implies better performance. We evaluate the overall performance of different bronze ware dating methods using overall accuracy (OA) and assess their individual performance at various levels of granularity using independent accuracy.

4.3. Bronze Ware Dating

Setting. We select five representative FGVC methods and one bronze ware dating method to evaluate their performance on the ShiftedBronzes dataset. Based on the experimental settings in [111], we chose three multi-granularity FGVC methods (YourFL [13], HRN [14], AKG [111]) and three single-granularity FGVC methods (NTS-Net [102], SPS [41], P2PNet [101]) for the bronze ware dating task. Notably, AKG [111] is specifically designed for the dating of bronze artifacts

Table 2. The comparison of seven FGVC methods on the bronze ware dataset. In addition to the overall accuracy on the test set, we have also tested each accuracy of different independent era and bronze ware category. Bold indicates the best results.

Method		OA	Bronze Ware Category (Ding/Gui)										
			Shang		Western Zhou			Spring and Autumn			Warring States		
			Early	Late	Early	Mid	Late	Early	Mid	Late	Early	Mid	Late
Single-Granularity	NTS-Net [102]	73.19	82.35	73.58	79.27	74.58	79.55	61.47	55.34	71.31	30.23	35.9	71.83
	SPS [41]	75.74	82.35	79.72	79.27	76.04	76.3	70.18	58.25	68.85	51.16	35.9	83.1
	P2PNet [101]	76.03	88.24	70.05	84.75	75.42	75	81.65	53.4	75.41	48.84	41.03	88.73
Multi-Granularity	YourFL [13]	99.54	99.60/99.45										
		82.37	72.65		88.17			79.01			77.78		
		70.28	68.63	73.12	76.4	70.62	68.51	68.35	52.43	62.3	27.91	41.03	71.83
	HRN [14]	39.57	25.24/62.75										
		85.98	78.21		90.68			82.62			83.66		
		73.85	78.43	75.42	80.18	75.21	70.13	72.02	54.37	71.31	39.53	23.08	81.69
	AKG [111]	99.72	99.66/99.82										
		87.84	82.76		91.51			85.78			80.12		
	77.88	88.24	81.11	82.4	75.42	79.55	74.77	63.11	70.49	53.49	33.33	84.51	

Table 3. The comparison of eighteen OOD detection methods on the OOD data in ShiftedBronzes and five general OOD datasets. We categorized the comparative methods into three types based on their mechanisms and reported their FPR@95 and AUPOC. Bold red indicates the best performance, while underlined red denotes the second-best performance.

Method	Method Type	Sketch and Rubbing FPR@95, AUROC [†]	Transferred Bronze FPR@95, AUROC [†]	Transferred Container FPR@95, AUROC [†]	Container FPR@95, AUROC [†]	Species FPR@95, AUROC [†]	ImageNet-O FPR@95, AUROC [†]	iNaturalist FPR@95, AUROC [†]	Texture FPR@95, AUROC [†]	OpenImage-O FPR@95, AUROC [†]	Average FPR@95, AUROC [†]	
DICE [89]	Post-hoc Methods	98.30/26.74	75.11/67.79	94.15/37.35	88.69/52.48	84.24/57.12	90.93/44.59	93.41/31.69	92.60/45.89	93.15/41.30	90.07/45.11	
EBO [59]		89.27/58.15	70.51/75.45	61.41/80.54	64.86/78.95	45.40/88.15	59.26/82.93	56.91/74.61	86.27/69.51	60.61/79.88	65.83/76.46	
GradNorm [39]		89.16/57.53	64.02/77.46	65.27/79.56	53.92/84.05	38.78/90.71	52.93/84.63	52.86/77.49	83.72/67.14	57.23/81.31	62.21/77.76	
Gram [78]		83.83/28.37	95.24/50.25	87.20/61.75	78.52/68.92	80.13/77.78	87.14/68.33	74.95/65.27	83.76/69.40	85.69/64.68	84.05/61.64	
KL-Matching [6]		95.88/43.43	95.47/60.14	96.17/52.77	97.43/50.18	96.33/65.96	96.30/60.98	97.75/41.62	96.66/54.15	96.72/55.56	96.52/53.87	
KNN [90]		89.26/58.54	60.06/81.07	45.40/86.94	40.93/89.39	17.81/95.98	22.09/94.61	18.65/94.10	28.04/93.03	22.35/94.56	38.29/87.58	
MDS [51]		93.73/57.11	66.23/87.03	22.44/92.20	14.39/95.17	10.03/96.95	7.11/98.11	1.64/99.48	1.83/99.61	6.88/98.24	21.79/1.56	
MLS [6]		87.27/58.24	70.51/75.29	61.48/80.14	65.02/78.66	45.66/87.82	59.42/82.64	56.91/74.43	86.27/69.61	60.68/79.67	65.91/76.28	
MSP [37]		88.78/60.35	72.15/71.39	68.55/71.57	68.55/72.17	54.57/80.32	63.76/76.17	64.02/69.84	75.56/71.23	63.73/74.39	68.85/71.94	
ODIN [56]		55.34/85.02	80.87/72.90	77.52/81.14	88.52/82.01	80.48/82.88	94.50/74.69	79.61/81.23	96.40/71.88	87.91/79.27	82.35/79.0	
OpenMax [8]		89.84/62.33	73.41/69.93	70.00/72.64	70.03/69.85	55.50/79.80	64.86/76.79	65.24/69.78	74.60/71.81	64.69/74.91	69.87/1.98	
ReAct [88]		87.30/54.94	64.89/77.34	63.76/78.80	65.18/78.66	47.52/87.17	60.55/81.34	58.97/72.51	87.78/68.41	61.32/78.42	66.36/75.29	
VIM [94]		86.43/55.05	<u>38.78/90.60</u>	22.77/94.89	<u>17.94/96.30</u>	4.47/98.97	4.47/98.96	1.41/99.72	<u>1.29/99.59</u>	4.50/99.03	20.23/92.57	
OpenGAN [45]		Generation-based Methods	50.44/81.32	79.18/58.59	45.57/82.24	43.36/78.25	45.74/72.27	48.55/74.51	39.33/81.56	71.89/73.95	45.78/76.9	52.27/5.07
DIFFGUARD [27]			32.49/82.42	97.93/34.6	97.16/40.22	98.07/19.51	99.59/7.69	86.84/47.16	61.85/72.54	70.97/61.25	95.19/30.07	82.78/44.49
LoCoOp [69]		VLM-based Methods	53.72/84.71	47.94/86.24	64.29/74.86	41.85/86.77	61.97/82.67	41.83/88.19	90.44/55.91	20.09/61.16	61.06/76.48	53.88/1.11
ID-like [5]			24.55/94.04	5.13/98.8	22.22/41.43	0.55/99.79	0.07/99.93	0.03/99.95	0.09/99.99	0.09/99.98	0.23/99.92	5.32/98.64
CLIPN [93]			58.55/82.87	48.82/80.61	69.65/69.34	7.75/97.72	7.25/98.11	7.71/98.12	21.82/94.26	8.46/97.59	13.53/96.25	27.06/90.54

Results and Analysis. (1) *Domain-specific expert knowledge significantly enhances the model learning for bronze ware dating.* As can be seen from Table 2, the AKG achieves the best OA performance. Moreover, it also attains the best independent accuracy across two bronze ware categories, three coarse-granularity eras and five fine-granularity eras. Designed with the dating of bronze Ding, the AKG outperform other general FGVC methods even when applied to the expanded data with Gui. (2) *Multi-level feature enhancement does not always yield effective improvements.* Except for the top-performing AKG, the other two multi-granularity FGVC methods underperform compared to SPS and P2PNet. And the performance of HRN on bronze ware category classification is significantly lower than that of other multi-granularity methods. This indicates that merely obtaining additional information from hierarchical labels is insufficient, and multi-granularity features may interfere with each other.

4.4. OOD Detection Experiments

4.4.1. Setting

We selected eighteen widely studied OOD detection methods, which are divided into three categories (post-hoc, VLM-based, generation-based), and conducted OOD detection experiments on ShiftedBronzes dataset, as well as five general OOD datasets. The post-hoc methods include DICE [89], EBO [59], GradNorm [39], Gram [78], KL-Matching [6], KNN [90], MDS [51], MLS [6], MSP [37], ODIN [56], OpenMax [8], ReAct [88] and VIM [94]. We selected the AKG, which demonstrated the best performance in the bronze ware dating experiments, to serve as the pre-model for post-hoc methods.

The VLM-based methods include ID-like [5], LoCoOp [69] and CLIPN [93]. ID-like [5] and LoCoOp [69] employ few-shot prompt learning for training. We conducted experiments to evaluate their performance under varying numbers of training samples and selected the best-performing configurations to compared with other methods. CLIPN [93] has been pre-training on the CC3M [81] dataset, followed by zero-shot inference.

The generation-based methods include OpenGAN [45]

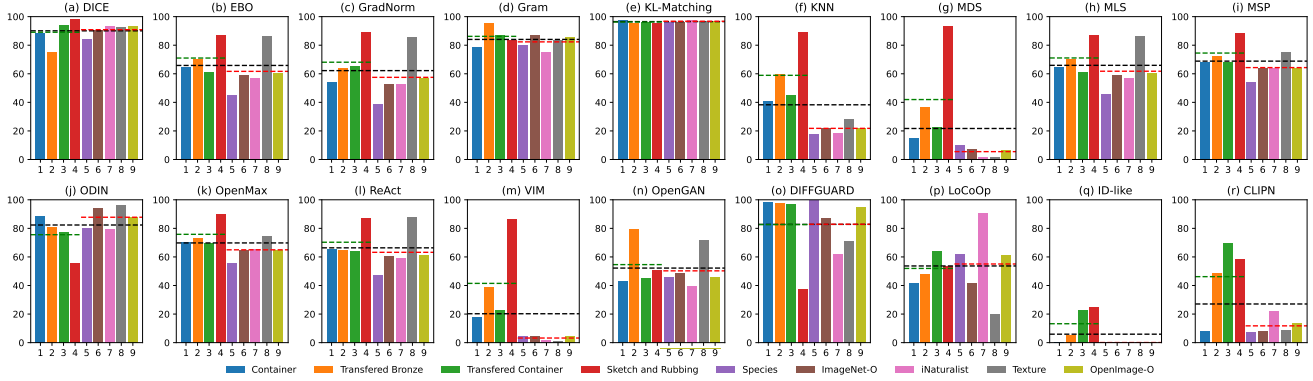


Figure 5. The comparison of FPR@95 performance of 18 OOD detection methods on the OOD data in ShiftedBronzes and five general OOD datasets. The black dashed line represents the average performance across all OOD data. The green dashed line indicates the average performance on the *hard OOD data* (container, transferred bronze, transferred container, sketch and rubbing). The red dashed line indicates the average performance on the *easy OOD data* (Species, ImageNet-O, iNaturalist, Texture, OpenImage-O).

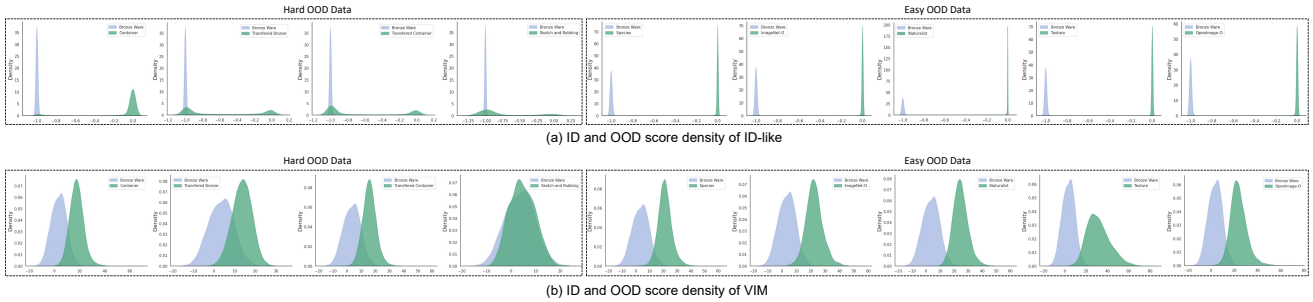


Figure 6. ID and OOD score density distribution of two top-performing methods on the *hard OOD data* and *easy OOD data*.

and DIFFGUARD [27]. The pre-model required by OpenGAN uses the same AKG as the post-hoc methods.

Table 4. Comparison of the average performance of post-hoc, VLM-based and generation-based methods.

	All OOD Data FPR@95↓ AUROC↑	Hard OOD Data FPR@95↓ AUROC↑	Easy OOD Data FPR@95↓ AUROC↑
Post-hoc	64.01/73.93	70.79/69.82	58.60/77.21
VLM-based	28.89/90.10	37.13/87.59	22.29/92.10
Generation-based	67.49/59.78	68.63/59.76	66.57/59.79

4.4.2. Results and Analysis

As shown in the red-marked metrics in Table 1, ID-like [5] and DIFFGUARD [27] achieved the top-2 average FPR@95 and AUROC performance on the sketch and rubbing data. On the transferred and container data, ID-like, MDS [51], and VIM [94] dominated the top-2 average FPR@95 and AUROC performance. For the general data, ID-like and VIM largely dominated the top-2 performances. Through further analysis of these methods across various OOD datasets, we derived some empirical findings, which we hope will contribute to the advancement of OOD detection algorithms for domain-specific data.

(1) *Pre-trained diffusion model-based methods are sensitive to color distribution shift.* DiffGuard and OpenGAN did not perform well on most of the other datasets. However, DiffGuard achieved performance just below ID-like [5] on the sketch and rubbing data, highlighting the potential of pre-trained diffusion models for detecting OOD samples with color distribution shifts. Analyzing the sensitivity of generation-based methods to color distribution shifts may provide insights for improving their performance on other datasets.

(2) *General knowledge in VLMs and proprietary knowledge in specialized datasets are key to VLM-based methods outperforming others.* VLMs are pre-trained in an open-world setting, which provides VLM-based methods with an inherent advantage in OOD detection. As shown in Figure 4, VLM-based methods outperform all others in terms of average performance across various OOD datasets and difficulty levels. Among the three VLM-based methods tested, ID-like [5] consistently achieved the best or second-best performance across all OOD data and average metrics. In contrast, CLIPN [93] and LoCoOp [69], although also based on VLMs, did not show any significant advantage.

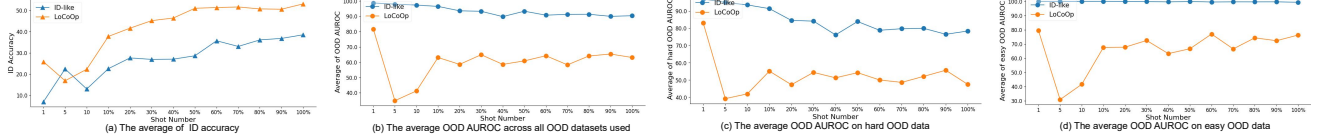


Figure 7. Comparison of ID and OOD performance of ID-like [5] and LoCoOp [69] under varying amounts of training data.

This can be attributed to differences in their prompt architectures: ID-like incorporates both learnable ID and OOD prompts, allowing it to leverage expert knowledge from ID samples. On the other hand, LoCoOp and CLIPN only have learnable OOD prompts, which limits their ability to capture ID-specific information. Furthermore, CLIPN’s pre-training on the CC3M dataset [81], which lacks domain-specific bronze ware data, further hinders its performance in bronze ware OOD detection.

(3) *ID and OOD performance variations during fine-tuning VLM-based methods with varying sample sizes differ across specialized and general domains.* We tested the ID and OOD performance of ID-like [5] and LoCoOp [69] methods with varying training sample sizes, as shown in Figure 7. Ming et al.[66] examined the effect of training sample size on the Caltech-101 dataset, finding that both ID and OOD performance improved as the sample size increased. However, our results on the ShiftedBronzes benchmark reveal a different trend. Both ID-like and LoCoOp demonstrated their best OOD detection performance with the 1-shot training paradigm. As the number of samples for fine-tuning increased, performance on *easy OOD data* with larger distribution shifts stabilized, while performance on *hard OOD data* with smaller shifts declined. This indicates that OOD detection in specialized domains, such as our proposed ShiftedBronzes, exhibits distinct patterns compared to general domain OOD detection, possibly due to more domain-specific characteristics.

(4) *Trainable ID prompts make the performance of VLM-based methods more stable.* Although the overall trend of LoCoOp [69] is similar to that of ID-like [5] when trained with different numbers of samples, it exhibits significant fluctuations, particularly when fewer samples are used. As shown in Figure 7(b-d), the performance of LoCoOp fluctuates noticeably as the number of training samples increases, with more pronounced fluctuations when fewer samples are used. In contrast, ID-like, which trains both ID and OOD prompts, shows more stable performance than LoCoOp, which trains only the OOD prompt. This offers insights for the design of VLM-based OOD detection methods.

(5) *Post-hoc methods that leverage diverse features throughout the pipeline, as well as those that can adaptively tune parameters of score function based on specialized domain data, often demonstrate superior performance.* Although post-hoc methods generally underperform VLM-

based methods, they offer greater flexibility and ease of deployment. Analyzing these methods is crucial for developing future approaches that may surpass VLM-based methods. As shown in Table 3, among post-hoc methods, MDS [51] and ViM [94] exhibit superior performance. MDS computes OOD scores using Mahalanobis distances and allows parameters of score function adjustment based on ID samples, which enhances robustness across different OOD datasets. ViM, on the other hand, combines softmax scores, logits, and residuals from the feature space to compute OOD scores, outperforming methods that rely on a single source of input, such as features (KNN [90]), max logits (MLS [6]), or max softmax (MSP [37]).

(6) *Compared to general OOD data, the smaller distribution shift in domain-specific OOD data poses a greater challenge for current OOD detection methods.* Compared to *easy OOD data*, *hard OOD data* exhibits a smaller distribution shift relative to ID data, a pattern also observed in other specialized domains. To explore the impact of distribution shifts on OOD detection performance, we compare the performance of various methods on both hard and *easy OOD data*. As shown in Figure 5, 13 out of the 18 methods evaluated show weaker average FRP@95 on *hard OOD data* than on *easy OOD data*. The top five methods in terms of average FRP@95 perform significantly worse on *hard OOD data* compared to *easy OOD data*. Notably, ID-like [5] and ViM [94] demonstrate the top-2 performance among the 18 methods. To further investigate, we plot the ID and OOD score density distributions for these two top-performing methods on the bronze ware test set, as well as on hard and *easy OOD data*, shown in Figure 6. The score density distributions for ID and *hard OOD data* exhibit significant overlap, while the distinction is clearer on the *easy OOD data*. These results suggest that top-performing OOD detection methods struggle with OOD samples that exhibit small distribution shifts relative to the ID data.

5. Limitations and Conclusion

There are several limitations in our study that should be addressed in future work. First, the lack of data from other specialized domains may limit the generalizability of our findings. Additionally, our comparison does not cover all types of OOD detection methods, which could affect the comprehensiveness of our conclusions.

In this study, we introduce a novel benchmark Shifted-

Bronzes to assess the dating of bronze wares amidst diverse domain distribution shifts within open-world scenarios. With a thorough comparison of six FGVC and eighteen OOD detection methods, we demonstrate that bronze ware dating with domain distribution shifts remains a challenge and requires further attention from the research community. Furthermore, we empirically investigate how OOD performance in specialized domain is influenced by various factors, including distribution shift types, detector architecture, pre-training, etc. We hope our research can contribute to both the archaeology and the development of OOD detection algorithms.

References

- [1] Alpher, F. (2002). Frobnication. *IEEE TPAMI*, 12(1):234–778.
- [2] Alpher, F. and Fotheringham-Smythe, F. (2003). Frobnication revisited. *Journal of Foo*, 13(1):234–778.
- [3] Alpher, F., Fotheringham-Smythe, F., and Gamow, F. (2004). Can a machine frobnicate? *Journal of Foo*, 14(1):234–778.
- [4] Alpher, F. and Gamow, F. (2005). Can a computer frobnicate? In *CVPR*, pages 234–778.
- [5] Bai, Y., Han, Z., Cao, B., Jiang, X., Hu, Q., and Zhang, C. (2024). Id-like prompt learning for few-shot out-of-distribution detection. In *Proceedings of the IEEE/CVF Conference on Computer Vision and Pattern Recognition*, pages 17480–17489. 3, 6, 7, 8
- [6] Basart, S., Mantas, M., Mohammadreza, M., Jacob, S., and Dawn, S. (2022). Scaling out-of-distribution detection for real-world settings. In *International Conference on Machine Learning*. 5, 6, 8
- [7] Ben-David, S., Blitzer, J., Crammer, K., Kulesza, A., Pereira, F., and Vaughan, J. W. (2010). A theory of learning from different domains. *Machine learning*, 79:151–175.
- [8] Bendale, A. and Boulton, T. E. (2016). Towards open set deep networks. In *Proceedings of the IEEE conference on computer vision and pattern recognition*, pages 1563–1572. 6
- [9] Borlino, F. C., Lu, L., and Tommasi, T. (2024). Foundation models and fine-tuning: A benchmark for out of distribution detection. *IEEE Access*.
- [10] Cao, T., Huang, C.-W., Hui, D. Y.-T., and Cohen, J. P. (2020). A benchmark of medical out of distribution detection. *arXiv preprint arXiv:2007.04250*. 2, 3
- [11] CAPPIO BORLINO, F. (2024). Addressing distributional shift challenges in computer vision for real-world applications.
- [12] Cerri, R., Barros, R. C., PLF de Carvalho, A. C., and Jin, Y. (2016). Reduction strategies for hierarchical multi-label classification in protein function prediction. *BMC bioinformatics*, 17(1):1–24.
- [13] Chang, D., Pang, K., Zheng, Y., Ma, Z., Song, Y.-Z., and Guo, J. (2021). Your” flamingo” is my” bird”: Fine-grained, or not. In *Proceedings of the IEEE/CVF Conference on Computer Vision and Pattern Recognition*, pages 11476–11485. 3, 5, 6
- [14] Chen, J., Wang, P., Liu, J., and Qian, Y. (2022). Label relation graphs enhanced hierarchical residual network for hierarchical multi-granularity classification. In *Proceedings of the IEEE/CVF Conference on Computer Vision and Pattern Recognition*, pages 4858–4867. 3, 5, 6
- [15] Chen, T., Wu, W., Gao, Y., Dong, L., Luo, X., and Lin, L. (2018). Fine-grained representation learning and recognition by exploiting hierarchical semantic embedding. In *Proceedings of the 26th ACM international conference on Multimedia*, pages 2023–2031.
- [16] Cheng, T.-Y., Sharma, P., Markham, A., Trigoni, N., and Jampani, V. (2025). Zest: Zero-shot material transfer from a single image. In *European Conference on Computer Vision*, pages 370–386. Springer. 5
- [17] Deng, J., Ding, N., Jia, Y., Frome, A., Murphy, K., Bengio, S., Li, Y., Neven, H., and Adam, H. (2014). Large-scale object classification using label relation graphs. In *European conference on computer vision*, pages 48–64. Springer.
- [18] Deng, J., Dong, W., Socher, R., Li, L.-J., Li, K., and Fei-Fei, L. (2009). Imagenet: A large-scale hierarchical image database. In *2009 IEEE conference on computer vision and pattern recognition*, pages 248–255. Ieee.
- [19] Doménech-Carbó, A., Doménech-Carbó, M., Redondo-Marugán, J., Osete-Cortina, L., Barrio, J., Fuentes, A., Vivancos-Ramón, M., Al Sekhaneh, W., Martínez, B., Martínez-Lázaro, I., et al. (2018). Electrochemical characterization and dating of archaeological leaded bronze objects using the voltammetry of immobilized particles. *Archaeometry*, 60(2):308–324. 3
- [20] Doménech-Carbó, A., Doménech-Carbó, M. T., Capelo, S., Pasfies, T., and Martínez-Lázaro, I. (2014). Dating archaeological copper/bronze artifacts by using the voltammetry of microparticles. *Angewandte Chemie*, 126(35):9416–9420. 3
- [21] Dosovitskiy, A., Beyer, L., Kolesnikov, A., Weissenborn, D., Zhai, X., Unterthiner, T., Dehghani, M., Minderer, M., Heigold, G., Gelly, S., Uszkoreit, J., and Houshy, N. (2021). An image is worth 16x16 words: Transformers for image recognition at scale. In *International Conference on Learning Representations*. 5
- [22] Drummond, N. and Shearer, R. (2006). The open world assumption. In *eSI Workshop: The Closed World of Databases meets the Open World of the Semantic Web*, volume 15, page 1.
- [23] Du, X., Sun, Y., Zhu, J., and Li, Y. (2024). Dream the impossible: Outlier imagination with diffusion models. *Advances in Neural Information Processing Systems*, 36. 3
- [24] Dubey, A., Gupta, O., Guo, P., Raskar, R., Farrell, R., and Naik, N. (2018a). Pairwise confusion for fine-grained visual classification. In *Proceedings of the European conference on computer vision (ECCV)*, pages 70–86.
- [25] Dubey, A., Gupta, O., Raskar, R., and Naik, N. (2018b). Maximum-entropy fine grained classification. *Advances in neural information processing systems*, 31.
- [26] Galil, I., Dabbah, M., and El-Yaniv, R. (2023). A framework for benchmarking class-out-of-distribution detection and its application to imagenet. In *The Eleventh International Conference on Learning Representations*.
- [27] Gao, R., Zhao, C., Hong, L., and Xu, Q. (2023). Diffguard: Semantic mismatch-guided out-of-distribution detection using pre-trained diffusion models. In *Proceedings of the IEEE/CVF International Conference on Computer Vision*, pages 1579–1589. 3, 6, 7

- [28] Gardner, J., Popovic, Z., and Schmidt, L. (2024). Benchmarking distribution shift in tabular data with tablesift. *Advances in Neural Information Processing Systems*, 36.
- [29] Giunchiglia, E. and Lukasiewicz, T. (2020). Coherent hierarchical multi-label classification networks. *Advances in Neural Information Processing Systems*, 33:9662–9673.
- [30] Graham, M. S., Pinaya, W. H., Tudosiu, P.-D., Nachev, P., Ourselin, S., and Cardoso, J. (2023). Denoising diffusion models for out-of-distribution detection. In *Proceedings of the IEEE/CVF Conference on Computer Vision and Pattern Recognition*, pages 2948–2957. 3
- [31] Greenacre, M. and Wood, J. R. (2024). A comprehensive workflow for compositional data analysis in archaeometry, with code in r. *Archaeological and Anthropological Sciences*, 16(10):171.
- [32] Gui, S., Li, X., Wang, L., and Ji, S. (2022). Good: A graph out-of-distribution benchmark. *Advances in Neural Information Processing Systems*, 35:2059–2073.
- [33] He, J., Zhu, Q., Chen, Y., and Nie, F. (2020). Bronze inscriptions classification algorithm on imbalanced dataset. In *2020 5th International Conference on Mechanical, Control and Computer Engineering (ICMCCE)*, pages 1715–1718. IEEE.
- [34] He, K., Zhang, X., Ren, S., and Sun, J. (2015). Delving deep into rectifiers: Surpassing human-level performance on imagenet classification. In *Proceedings of the IEEE international conference on computer vision*, pages 1026–1034. 2
- [35] He, K., Zhang, X., Ren, S., and Sun, J. (2016a). Deep residual learning for image recognition. In *Proceedings of the IEEE conference on computer vision and pattern recognition*, pages 770–778.
- [36] He, K., Zhang, X., Ren, S., and Sun, J. (2016b). Deep residual learning for image recognition. In *Proceedings of the IEEE conference on computer vision and pattern recognition*, pages 770–778. 5
- [37] Hendrycks, D. and Gimpel, K. (2017). A baseline for detecting misclassified and out-of-distribution examples in neural networks. In *International Conference on Learning Representations*. 3, 6, 8
- [38] Hendrycks, D., Zhao, K., Basart, S., Steinhardt, J., and Song, D. (2021). Natural adversarial examples. In *Proceedings of the IEEE/CVF conference on computer vision and pattern recognition*, pages 15262–15271. 5
- [39] Huang, R., Geng, A., and Li, Y. (2021a). On the importance of gradients for detecting distributional shifts in the wild. *Advances in Neural Information Processing Systems*, 34:677–689. 3, 6
- [40] Huang, R. and Li, Y. (2021). Mos: Towards scaling out-of-distribution detection for large semantic space. In *Proceedings of the IEEE/CVF Conference on Computer Vision and Pattern Recognition*, pages 8710–8719. 5
- [41] Huang, S., Wang, X., and Tao, D. (2021b). Stochastic partial swap: Enhanced model generalization and interpretability for fine-grained recognition. In *Proceedings of the IEEE/CVF International Conference on Computer Vision*, pages 620–629. 3, 5, 6
- [42] Huang, S., Xu, Z., Tao, D., and Zhang, Y. (2016). Part-stacked cnn for fine-grained visual categorization. In *Proceedings of the IEEE conference on computer vision and pattern recognition*, pages 1173–1182.
- [43] Humblot-Renaux, G., Escalera, S., and Moeslund, T. B. (2024). A noisy elephant in the room: Is your out-of-distribution detector robust to label noise? In *Proceedings of the IEEE/CVF Conference on Computer Vision and Pattern Recognition*, pages 22626–22636.
- [44] Ji, Y., Zhang, L., Wu, J., Wu, B., Huang, L.-K., Xu, T., Rong, Y., Li, L., Ren, J., Xue, D., et al. (2022). Drugood: Out-of-distribution (ood) dataset curator and benchmark for ai-aided drug discovery—a focus on affinity prediction problems with noise annotations. *arXiv preprint arXiv:2201.09637*. 2, 3
- [45] Kong, S. and Ramanan, D. (2021). Opengan: Open-set recognition via open data generation. In *Proceedings of the IEEE/CVF International Conference on Computer Vision*, pages 813–822. 3, 6
- [46] Krizhevsky, A., Sutskever, I., and Hinton, G. E. (2012). Imagenet classification with deep convolutional neural networks. *Advances in neural information processing systems*, 25. 2
- [47] Kuang, B., Chen, Y., and Su, B. (2020). Detecting for bronze inscriptions. In *Proceedings of the 2020 4th International Conference on Electronic Information Technology and Computer Engineering*, pages 555–559.
- [48] Kylberg, G. (2011). *Kylberg texture dataset v. 1.0*. Centre for Image Analysis, Swedish University of Agricultural Sciences and . . . 5
- [49] LastName, F. (2014a). The frobnicable foo filter. Face and Gesture submission ID 324. Supplied as supplemental material fg324.pdf.
- [50] LastName, F. (2014b). Frobnication tutorial. Supplied as supplemental material tr.pdf.
- [51] Lee, K., Lee, K., Lee, H., and Shin, J. (2018). A simple unified framework for detecting out-of-distribution samples and adversarial attacks. *Advances in neural information processing systems*, 31. 3, 6, 7, 8
- [52] Li, C., Qi, R., Tang, C., Wei, J., Yang, X., Zhang, Q., and Zhou, R. (2023). Ai mobile application for archaeological dating of bronze dings. *arXiv preprint arXiv:2401.01002*. 3
- [53] Li, D., Yang, Y., Song, Y.-Z., and Hospedales, T. M. (2017). Deeper, broader and artier domain generalization. In *Proceedings of the IEEE international conference on computer vision*, pages 5542–5550.
- [54] Li, F., Andreeto, M., Ranzato, M., and Perona, P. (2022). Caltech 101 (1.0)[data set]. caltechdata.
- [55] Li, L., Wang, Y., Sitawarin, C., and Spratling, M. (2024). OODRobustbench: a benchmark and large-scale analysis of adversarial robustness under distribution shift. In *ICLR 2024 Workshop on Data-centric Machine Learning Research (DMLR): Harnessing Momentum for Science*. 2, 3
- [56] Liang, S., Li, Y., and Srikant, R. (2018). Enhancing the reliability of out-of-distribution image detection in neural networks. In *International Conference on Learning Representations*. 3, 6
- [57] Lin, T.-Y., RoyChowdhury, A., and Maji, S. (2015). Bilinear cnn models for fine-grained visual recognition. In *Proceedings of the IEEE international conference on computer vision*, pages 1449–1457.

- [58] Ling, H., Qingrong, Z., and Min, G. (2007). Characterization of corroded bronze ding from the yin ruins of china. *Corrosion science*, 49(6):2534–2546. 3
- [59] Liu, W., Wang, X., Owens, J., and Li, Y. (2020). Energy-based out-of-distribution detection. *Advances in neural information processing systems*, 33:21464–21475. 3, 6
- [60] Liu, X. (2014). Identification and collection of bronze dings of all ages. *Oriental Collection*, (8):121–124.
- [61] Liu, Z., Luo, P., Qiu, S., Wang, X., and Tang, X. (2016). Large-scale fashion (deepfashion) database. *Xiaoou Tang Multimedia Laboratory, The Chinese University of Hong Kong, Category and Attribute Prediction Benchmark*. <https://url.kr/dfQWIV>. 5
- [62] Lotfollahi, M., Naghipourfar, M., Theis, F. J., and Wolf, F. A. (2020). Conditional out-of-distribution generation for unpaired data using transfer vae. *Bioinformatics*, 36(Supplement_2):i610–i617.
- [63] Luo, W., Yang, X., Mo, X., Lu, Y., Davis, L. S., Li, J., Yang, J., and Lim, S.-N. (2019). Cross-x learning for fine-grained visual categorization. In *Proceedings of the IEEE/CVF international conference on computer vision*, pages 8242–8251.
- [64] Mao, X., Chen, Y., Zhu, Y., Chen, D., Su, H., Zhang, R., and Xue, H. (2023). Coco-o: A benchmark for object detectors under natural distribution shifts. In *Proceedings of the IEEE/CVF International Conference on Computer Vision*, pages 6339–6350. 3
- [65] Ming, Y., Cai, Z., Gu, J., Sun, Y., Li, W., and Li, Y. (2022). Delving into out-of-distribution detection with vision-language representations. *Advances in neural information processing systems*, 35:35087–35102. 3
- [66] Ming, Y. and Li, Y. (2024). How does fine-tuning impact out-of-distribution detection for vision-language models? *International Journal of Computer Vision*, 132(2):596–609. 8
- [67] Mirzaei, H., Salehi, M., Shahabi, S., Gavves, E., Snoek, C. G., Sabokrou, M., and Rohban, M. H. (2022). Fake it until you make it: Towards accurate near-distribution novelty detection. In *The eleventh international conference on learning representations*. 3
- [68] Misra, I., Shrivastava, A., Gupta, A., and Hebert, M. (2016). Cross-stitch networks for multi-task learning. In *Proceedings of the IEEE conference on computer vision and pattern recognition*, pages 3994–4003.
- [69] Miyai, A., Yu, Q., Irie, G., and Aizawa, K. (2024). Locoop: Few-shot out-of-distribution detection via prompt learning. *Advances in Neural Information Processing Systems*, 36. 3, 6, 7, 8
- [70] Moonshot AI Technology Co., L. (2024). Kimi: Your ai companion. <https://moonshot.cn/kimi>. Accessed: 2024-11-11. 4
- [71] Nascetti, A., Yadav, R., Brodt, K., Qu, Q., Fan, H., Shendryk, Y., Shah, I., and Chung, C. (2024). Biomasters: A benchmark dataset for forest biomass estimation using multi-modal satellite time-series. *Advances in Neural Information Processing Systems*, 36.
- [72] Omeo, S. S., Fu, N., Dong, R., Hu, M., and Hu, J. (2024). Structure-based out-of-distribution (ood) materials property prediction: a benchmark study. *npj Computational Materials*, 10(1):144. 2, 3
- [73] Radford, A., Kim, J. W., Hallacy, C., Ramesh, A., Goh, G., Agarwal, S., Sastry, G., Askell, A., Mishkin, P., Clark, J., et al. (2021). Learning transferable visual models from natural language supervision. In *International conference on machine learning*, pages 8748–8763. PMLR. 3
- [74] Ridnik, T., Ben-Baruch, E., Noy, A., and Zelnik-Manor, L. (2021). Imagenet-21k pretraining for the masses. In *Thirty-fifth Conference on Neural Information Processing Systems Datasets and Benchmarks Track (Round 1)*. 1
- [75] Ruff, L., Kauffmann, J. R., Vandermeulen, R. A., Montavon, G., Samek, W., Kloft, M., Dietterich, T. G., and Müller, K.-R. (2021). A unifying review of deep and shallow anomaly detection. *Proceedings of the IEEE*, 109(5):756–795.
- [76] Ruiz, N., Li, Y., Jampani, V., Pritch, Y., Rubinstein, M., and Aberman, K. (2023). Dreambooth: Fine tuning text-to-image diffusion models for subject-driven generation. In *Proceedings of the IEEE/CVF conference on computer vision and pattern recognition*, pages 22500–22510.
- [77] Saharia, C., Chan, W., Saxena, S., Li, L., Whang, J., Denton, E. L., Ghasemipour, K., Gontijo Lopes, R., Karagol Ayan, B., Salimans, T., et al. (2022). Photorealistic text-to-image diffusion models with deep language understanding. *Advances in neural information processing systems*, 35:36479–36494.
- [78] Sastry, C. S. and Oore, S. (2020). Detecting out-of-distribution examples with Gram matrices. In III, H. D. and Singh, A., editors, *Proceedings of the 37th International Conference on Machine Learning*, volume 119 of *Proceedings of Machine Learning Research*, pages 8491–8501. PMLR. 3, 6
- [79] Schlegl, T., Seeböck, P., Waldstein, S. M., Schmidt-Erfurth, U., and Langs, G. (2017). Unsupervised anomaly detection with generative adversarial networks to guide marker discovery. In *International conference on information processing in medical imaging*, pages 146–157. Springer. 3
- [80] Serrà, J., Álvarez, D., Gómez, V., Slizovskaia, O., Núñez, J. F., and Luque, J. (2020). Input complexity and out-of-distribution detection with likelihood-based generative models. In *International Conference on Learning Representations*. 3
- [81] Sharma, P., Ding, N., Goodman, S., and Soricut, R. (2018). Conceptual captions: A cleaned, hypernymed, image alt-text dataset for automatic image captioning. In *Proceedings of the 56th Annual Meeting of the Association for Computational Linguistics (Volume 1: Long Papers)*, pages 2556–2565. 6, 8
- [82] Shi, J., Gare, G. R., Tian, J., Chai, S., Lin, Z., Vasudevan, A. B., Feng, D., Ferroni, F., Kong, S., and Ramanan, D. (2024). LCA-on-the-line: Benchmarking out of distribution generalization with class taxonomies. In *NeurIPS 2023 Workshop on Distribution Shifts: New Frontiers with Foundation Models*.
- [83] Shi, X. and Lee, S. (2024). Benchmarking out-of-distribution detection in visual question answering. In *Proceedings of the IEEE/CVF Winter Conference on Applications of Computer Vision*, pages 5485–5495.
- [84] Sickman, L. (1948). A descriptive and illustrative catalogue of chinese bronzes acquired during the administration of john ellerton lodge.
- [85] Simonyan, K. and Zisserman, A. (2014). Very deep convolutional networks for large-scale image recognition. *arXiv preprint arXiv:1409.1556*.

- [86] Sricharan, K. and Srivastava, A. (2018). Building robust classifiers through generation of confident out of distribution examples. *NeurIPS-W*. 3
- [87] Sun, M., Yuan, Y., Zhou, F., and Ding, E. (2018). Multi-attention multi-class constraint for fine-grained image recognition. In *Proceedings of the European Conference on Computer Vision (ECCV)*, pages 805–821.
- [88] Sun, Y., Guo, C., and Li, Y. (2021). React: Out-of-distribution detection with rectified activations. *Advances in Neural Information Processing Systems*, 34:144–157. 6
- [89] Sun, Y. and Li, Y. (2022). Dice: Leveraging sparsification for out-of-distribution detection. In *European Conference on Computer Vision*, pages 691–708. 3, 6
- [90] Sun, Y., Ming, Y., Zhu, X., and Li, Y. (2022). Out-of-distribution detection with deep nearest neighbors. In *International Conference on Machine Learning*, pages 20827–20840. PMLR. 6, 8
- [91] Vaze, S., Han, K., Vedaldi, A., and Zisserman, A. (2022). Open-set recognition: A good closed-set classifier is all you need? In *International Conference on Learning Representations (ICLR)*.
- [92] Vernekar, S., Gaurav, A., Abdelzad, V., Denouden, T., Salay, R., and Czarnecki, K. (2019). Out-of-distribution detection in classifiers via generation. *NeurIPS-W*. 3
- [93] Wang, H., Li, Y., Yao, H., and Li, X. (2023). Clipn for zero-shot ood detection: Teaching clip to say no. In *Proceedings of the IEEE/CVF International Conference on Computer Vision*, pages 1802–1812. 3, 6, 7
- [94] Wang, H., Li, Z., Feng, L., and Zhang, W. (2022). Vim: Out-of-distribution with virtual-logit matching. In *Proceedings of the IEEE/CVF conference on computer vision and pattern recognition*, pages 4921–4930. 1, 2, 5, 6, 7, 8
- [95] Wang, S., Chen, G., and Zhang, C. (2019). A study of the phasing and dating of western zhou bronzes. *Artifacts*, (9):96–96.
- [96] Wang, Y., Wei, G., Li, Q., Zheng, X., and Wang, D. (2021). Provenance of zhou dynasty bronze vessels unearthed from zongyang county, anhui province, china: determined by lead isotopes and trace elements. *Heritage Science*, 9(1):1–12. 3
- [97] Wei, X.-S., Song, Y.-Z., Mac Aodha, O., Wu, J., Peng, Y., Tang, J., Yang, J., and Belongie, S. (2021). Fine-grained image analysis with deep learning: A survey. *IEEE Transactions on Pattern Analysis and Machine Intelligence*.
- [98] Wei, X.-S., Xie, C.-W., Wu, J., and Shen, C. (2018). Mask-cnn: Localizing parts and selecting descriptors for fine-grained bird species categorization. *Pattern Recognition*, 76:704–714.
- [99] Wu, Z. (2012). A collection of shang and zhou bronze inscriptions and images. *Shanghai Ancient Books Publishing House*.
- [100] Yang, J., Wang, P., Zou, D., Zhou, Z., Ding, K., Peng, W., Wang, H., Chen, G., Li, B., Sun, Y., et al. (2022a). Openood: Benchmarking generalized out-of-distribution detection. *Advances in Neural Information Processing Systems*, 35:32598–32611. 2, 3, 5
- [101] Yang, X., Wang, Y., Chen, K., Xu, Y., and Tian, Y. (2022b). Fine-grained object classification via self-supervised pose alignment. In *Proceedings of the IEEE/CVF Conference on Computer Vision and Pattern Recognition*, pages 7399–7408. 3, 5, 6
- [102] Yang, Z., Luo, T., Wang, D., Hu, Z., Gao, J., and Wang, L. (2018). Learning to navigate for fine-grained classification. In *Proceedings of the European Conference on Computer Vision (ECCV)*, pages 420–435. 3, 5, 6
- [103] Yuan, L., Chen, Y., Cui, G., Gao, H., Zou, F., Cheng, X., Ji, H., Liu, Z., and Sun, M. (2023). Revisiting out-of-distribution robustness in nlp: Benchmarks, analysis, and llms evaluations. *Advances in Neural Information Processing Systems*, 36:58478–58507.
- [104] Zhang, C., Niwa, T., and Hirokawa, M. (2016a). On the piece mold-casting technology of the bronze gui-tureens in the shang and zhou dynasties. *Chinese Archaeology*, 16(1):162–167.
- [105] Zhang, H., Xu, T., Elhoseiny, M., Huang, X., Zhang, S., Elgammal, A., and Metaxas, D. (2016b). Spda-cnn: Unifying semantic part detection and abstraction for fine-grained recognition. In *Proceedings of the IEEE conference on computer vision and pattern recognition*, pages 1143–1152.
- [106] Zhang, N., Donahue, J., Girshick, R., and Darrell, T. (2014). Part-based r-cnns for fine-grained category detection. In *European conference on computer vision*, pages 834–849. Springer.
- [107] Zhao, B., Yu, S., Ma, W., Yu, M., Mei, S., Wang, A., He, J., Yuille, A., and Kortylewski, A. (2022). Ood-cv: A benchmark for robustness to individual nuisances in real-world out-of-distribution shifts. In *ICML 2022 Shift Happens Workshop*. 2, 3
- [108] Zhao, Y., Yan, K., Huang, F., and Li, J. (2021). Graph-based high-order relation discovery for fine-grained recognition. In *Proceedings of the IEEE/CVF Conference on Computer Vision and Pattern Recognition*, pages 15079–15088.
- [109] Zheng, Y., Yan, Y., and Qi, D. (2022). Bronze inscription recognition with distribution calibration based on few-shot learning. In *4th International Conference on Informatics Engineering & Information Science (ICIEIS2021)*, volume 12161, pages 150–158. SPIE.
- [110] Zhou, D.-W., Ye, H.-J., and Zhan, D.-C. (2021). Learning placeholders for open-set recognition. In *Proceedings of the IEEE/CVF conference on computer vision and pattern recognition*, pages 4401–4410. 3
- [111] Zhou, R., Wei, J., Zhang, Q., Qi, R., Yang, X., and Li, C. (2023). Multi-granularity archaeological dating of chinese bronze dings based on a knowledge-guided relation graph. In *Proceedings of the IEEE/CVF Conference on Computer Vision and Pattern Recognition*, pages 3103–3113. 1, 2, 3, 4, 5, 6